

# Fermi acceleration and suppression of Fermi acceleration in a time-dependent Lorentz Gas.

Diego F. M. Oliveira

*Max Planck Institute for Dynamics and Self-Organization – Bunsenstrasse 10 - D-37073 - Göttingen - Germany  
CAMTP - Center For Applied Mathematics and Theoretical Physics – University of Maribor - Krekova 2 - SI-2000 -  
Maribor - Slovenia.*

Jürgen Vollmer

*Max Planck Institute for Dynamics and Self-Organization – Bunsenstrasse 10 - D-37073 - Göttingen - Germany.*

Edson D. Leonel

*Departamento de Estatística, Matemática Aplicada e Computação – Instituto de Geociências e Ciências Exatas –  
Universidade Estadual Paulista –  
Av. 24A, 1515 – Bela Vista – CEP: 13506-900 – Rio Claro – SP – Brazil.*

---

## Abstract

We study some dynamical properties of a Lorentz gas. We have considered both the static and time dependent boundary. For the static case we have shown that the system has a chaotic component characterized with a positive Lyapunov Exponent. For the time-dependent perturbation we describe the model using a four-dimensional nonlinear map. The behaviour of the average velocity is considered in two situations (i) non-dissipative and (ii) dissipative. Our results show that the unlimited energy growth is observed for the non-dissipative case. However, when dissipation, via damping coefficients, is introduced the energy changes and the unlimited energy growth is suppressed. The behaviour of the average velocity is described using scaling approach.

*Keywords:* Billiard, Lorentz Gas, Lyapunov exponents, Fermi Acceleration, Scaling.

---

## 1. Introduction

The process in which a classical particle acquires unlimited energy growth from collisions with heavy boundaries, also called as phenomenon of Fermi acceleration, were first reported by Enrico Fermi [1] as an attempt to explain the acceleration of cosmic rays. He proposed that such behaviour was due to interaction between charged particles and time-dependent magnetic fields. Soon after [1] some alternative models have been proposed using different approaches with application in different fields of science including molecular physics [2], optics [3], nanostructures [4], quantum dots [5].

---

*Email addresses:* [diegofregolente@gmail.com](mailto:diegofregolente@gmail.com) (Diego F. M. Oliveira), [juergen.vollmer@ds.mpg.de](mailto:juergen.vollmer@ds.mpg.de) (Jürgen Vollmer), [edleonel@rc.unesp.br](mailto:edleonel@rc.unesp.br) (Edson D. Leonel)

*Preprint submitted to Elsevier*

November 4, 2018

One of the most studied versions of the problem is the well known one-dimensional Fermi-Ulam model (FUM) [6, 7, 8, 9, 10, 11, 12]. The model consists of a classical particle confined and bouncing between two rigid walls in which one of them is fixed and the other one moves according to a periodic function. It is well known that the phase space, in the absence of dissipation, shows a mixed structure in the sense that depending on the combinations of control parameters and initial conditions, both invariant spanning curves (also called as invariant tori), chaotic seas and Kolmogorov- Arnold-Moser (KAM) islands are all observed. An alternative model was latter proposed by Pustyl'nikov [13, 14]. Such system consists of a classical particle bouncing in a vertical moving platform under the effect of an external constant gravitational field [15, 16, 17, 18, 19, 20, 21]. Both models seems to be quite similar. However there are many differences between them. The main difference is, that in the FUM framework the Fermi acceleration is not observed. On the other hand, for specific combinations of both control parameters and initial conditions the phenomenon of unlimited energy growth can be observed in the bouncer model. This apparent contradictory result was latter discussed and explained by Lichtenberg and Lieberman [22, 23] and can be easily understood by looking at the space phase. The FUM has a set of invariant spanning curves limiting the size of the chaotic sea (as well as the particle's velocity), but such invariant tori, which could be interpreted as a barrier, they are not observed in the bouncer model and the energy grows unbounded. However, in two-dimensional systems it is not so simple to say if the phenomenon of Fermi acceleration will be observed or not. In this sense a conjecture was proposed by Loskutov-Ryabov-Akinshin (LRA) [24]. Such conjecture, known as LRA-conjecture, states that a chaotic componet in the phase space with static boundary is a sufficient condition to observe Fermi acceleration when a perturbation is introduced. Results that corroborate the validity of this conjecture include the time dependent oval billiard [25], stadium billiard [26].

When dissipation is introduce, it causes a drastic change on the phase space. Invariant spanning curves are destroyed. the elliptic fixed points turns into sinks and the chaotic sea is replaced by a chaotic attractor [27]. However, the influence of dissipation on the averave velocity is still not fully understood. It was discussed by Leonel [30] some results for a one-dimensional Fermi-Ulam model. It is well known that such system in its original formulation the particle do not have unlimited energy growth. If one consider the motion of the moving wall to be random the phenomenon of Fermi acceleration is observed. However, the introduction of inelastic collision is enough to suppress Fermi acceleration. Results considering also the one dimension Fermi-Ulam model under an external force of type sawtooth [31] under effects of dissipation generated from a sliding of a body against a rough surface has also been considered. The external perturbation of sawtooth type was chosen because the oscillating wall always gives energy to the particle after collisions. The main question is: Would it be possibel to suppress Fermi acceleration under the efect of dissipation generated from a sliding of a body against a rough surface? The answer is not so simple and it dependes on both, initial conditionand the combination of control parameters. It was observed that for a certain range of parameters Fermi acceleration indeed happen, however, it is supresses under specific conditions.

In this paper, we study the problem of a Lorentz Gas considering both the static and the time-dependent boundary. In the first part of our work we study the Lorentz Gas with static boundary. We derived a two dimensional nonlinear mapping that describes the dynamics of the model. We obtain the phase space and we show that it is chaotic with positive Lyapunov Exponent. Then, in the second part of our paper we introduce a time-dependent perturbation on the boundary. There are many different ways to introduce time dependent perturbation and the most common methods are: stochastic case, where the boundary changes according to a random

function [28] ; regular case, where the size of the boundary varies according to an harmonic law [29]. However, in both situations the center of mass it is assumed to be fixed. Now, for the first time, we introduce a different kind of time dependent perturbation for a Lorentz gas. We assume that the radius of the scatters are fixed and the center of mass changes according to an harmonic function. Our main goal in this part of our work is to verify the validity of the LRA conjecture, which is confirmed when we studied the behaviour of the average velocity for an ensemble of particles. Since the phenomenon of Fermi Acceleration is present in this model our next approach is to introduce dissipation into the model via damping coefficients and trying to understand what is the influence of dissipation on the particles behaviour. Our results allow us to confirm that when inelastic collisions is introduced into the model it is a sufficient condition to break down the phenomenon of Fermi acceleration. In both, conservative as well as dissipative case, we describes the behaviour of average velocity using scaling formalism.

The paper is organized as follows. In section 2 we describe how to obtain the two-dimensional mapping that describes the dynamics of the static system. Section 3 is devoted to discuss the time dependent model as well as our numerical results. Finally, conclusion and acknowledgments are drawn in section 4.

## 2. A static Lorentz Gas and the mapping

In this section we discuss all the details needed for the construction of a non-linear mapping that describes the dynamics of the problem. The model consists of a classical particle of mass  $m$  suffering elastic collisions with circular scatters (see Fig 1). We choose a triangular arrangement of the scatters (which also seems to be the Star of David if one connect circles 1,5 and 9 and 11,7 and 3) in order to avoid particles traveling infinitely far between collision and the fixed lattice spacing  $a$  to be twice the radius of the scatters,  $R=a/2$ . The system is described in terms of a two dimensional mapping  $\Xi(\theta_n, b_n) = (\theta_{n+1}, b_{n+1})$  where the dynamical variable  $\theta_n$  denotes the direction of the trajectory while  $b_n$  is the impact parameter. Given an initial condition  $(\theta_0, b_0)$ , the particle starts from the black circle (center in Fig. 1) and hit one of the 12 others circles. In this sense, we specify the scattered hit in the collision  $n+1$  by  $s_n = 0, \dots, 11$  and we introduce  $l(s_n)$  for the distance of this scatterer and the scatterer hit at the collision  $n+1$ .  $l(s_n)$  can assume the values of  $2a/\sqrt{3}$  and  $2a$  for even and odd values of  $s_n$ , respectively. Additionally, when the particle hits the boundary it is specularly reflected with the same absolute velocity. The particle does not suffer influences of any external field along its linear trajectory. From the green triangle in Fig 2 (a) one can easily verify

$$\sin(\theta_n - \frac{\pi s_n}{6}) = -\frac{(b_{n+1} - b_n)}{l(s_n)}. \quad (1)$$

Moreover, from Fig. 2 (b) one can find that

$$\alpha = \arcsin(-b_{n+1}/R), \quad (2)$$

$$\beta = \pi - 2\alpha, \quad (3)$$

$$\psi = 2\alpha - \theta_n, \quad (4)$$

$$\theta_{n+1} = \pi - 2\alpha + \theta_n. \quad (5)$$

Such a result allow us to obtain  $\theta_{n+1}$ ,

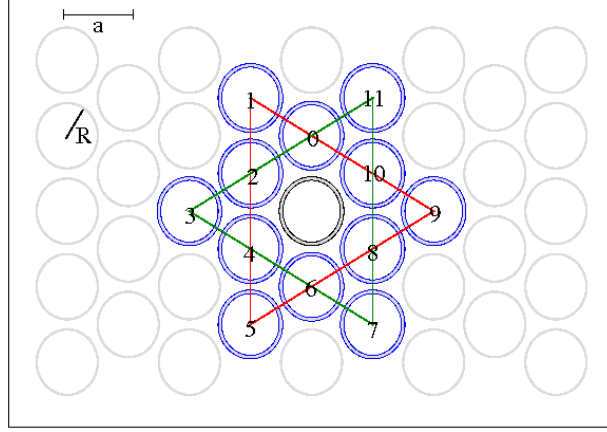


Figure 1: Illustration of the Lorentz gas with triangular configuration.

$$\theta_{n+1} = \pi + \theta_n + 2 \arcsin(b_{n+1}/R). \quad (6)$$

From Eq. 1 it is easily to find that the impact parameter,  $b_{n+1}$ , is given by

$$b_{n+1} = b_n - l(s_n) \sin(\theta_n - \frac{\pi s_n}{6}). \quad (7)$$

Thus, the mapping that describe the dynamics of a two dimensional Lorentz gas is given by

$$\Xi : \begin{cases} \theta_{n+1} = \pi + \theta_n + 2 \arcsin(\frac{b_{n+1}}{R}) \\ b_{n+1} = b_n - l(s_n) \sin(\theta_n - \frac{\pi s_n}{6}) \end{cases}, \quad (8)$$

by definition  $b \in [-R, R]$  and  $\theta \in [0, 2\pi]$  is a counterclockwise angle such that  $\Xi$  is defined on the fundamental domain  $[-R, R] \times [0, 2\pi]$ . From the mapping  $\Xi$ , Eq. (8), one can easily obtain the Jacobian Matrix,  $J$ , which is defined as

$$J = \begin{pmatrix} \frac{\partial \theta_{n+1}}{\partial \theta_n} & \frac{\partial \theta_{n+1}}{\partial b_n} \\ \frac{\partial b_{n+1}}{\partial \theta_n} & \frac{\partial b_{n+1}}{\partial b_n} \end{pmatrix}, \quad (9)$$

with coefficients given by

$$\frac{\partial \theta_{n+1}}{\partial \theta_n} = 1 - 2 \sqrt{R^2 - b_{n+1}^2} l(s_n) \cos(\theta_n - \frac{\pi s_n}{6}), \quad (10)$$

$$\frac{\partial \theta_{n+1}}{\partial b_n} = 2 \sqrt{R^2 - b_{n+1}^2}, \quad (11)$$

$$\frac{\partial b_{n+1}}{\partial \theta_n} = -l(s_n) \cos(\theta_n - \frac{\pi s_n}{6}), \quad (12)$$

$$\frac{\partial b_{n+1}}{\partial b_n} = 1. \quad (13)$$

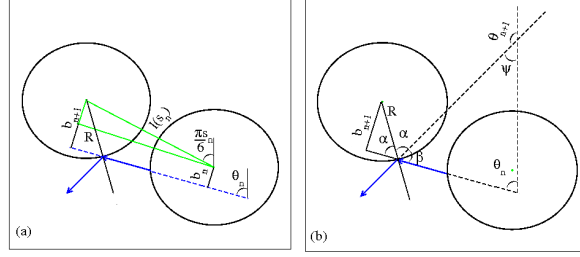


Figure 2: Dependence of (a)  $b_{n+1}$  on  $b_n$  and  $\theta_n$ ; (b)  $\theta_{n+1}$  on  $b_{n+1}$  and  $\theta_n$ .

After some easy calculation one can show that the mapping  $\Xi$  preserves the phase space measure since  $\det(J) = 1$ .

It is well known the Lyapunov exponents are an important tool to identify whether the model is chaotic or not. As discussed in [32], the Lyapunov exponents are defined as

$$\lambda_j = \lim_{n \rightarrow \infty} \frac{1}{n} \ln |\Lambda_j|, \quad j = 1, 2, \quad (14)$$

where  $\Lambda_j$  are the eigenvalues of  $M = \prod_{i=1}^n J_i(\theta_i, b_i)$  and  $J_i$  is the Jacobian matrix evaluated over the orbit  $(\theta_i, b_i)$ . However, a direct implementation of a computational algorithm to evaluate Eq. (14) has a severe limitation to obtain  $M$ . Even in the limit of short  $n$ , the components of  $M$  can assume very different orders of magnitude for chaotic orbits and periodic attractors yielding impracticable the implementation of the algorithm. In order to avoid such problem we note that  $J$  can be written as  $J = \Theta T$  where  $\Theta$  is an orthogonal matrix and  $T$  is a right triangular matrix. Thus we rewrite  $M$  as  $M = J_n J_{n-1} \dots J_2 \Theta_1 \Theta_1^{-1} J_1$ , where  $T_1 = \Theta_1^{-1} J_1$ . A product of  $J_2 \Theta_1$  defines a new  $J'_2$ . In a next step, it is easy to show that  $M = J_n J_{n-1} \dots J_3 \Theta_2 \Theta_2^{-1} J'_2 T_1$ . The same procedure can be used to obtain  $T_2 = \Theta_2^{-1} J'_2$  and so on. Using this procedure the problem is reduced to evaluate the diagonal elements of  $T_i : T_{11}^i, T_{22}^i$ . Finally, the Lyapunov exponents are now given by

$$\lambda_j = \lim_{n \rightarrow \infty} \frac{1}{n} \sum_{i=1}^n \ln |T_{jj}^i|, \quad j = 1, 2. \quad (15)$$

If at least one of the  $\lambda_j$  is positive then the orbit is classified as chaotic. Additionally, in conservative systems  $\lambda_1 + \lambda_2 = 0$  and in dissipative systems  $\lambda_1 + \lambda_2 < 0$ . The phase space for the mapping (8) is shown in Fig. 3(a). For the same control parameters used in Fig. 3 (a),  $a = 2$ , we have also evaluated numerically the positive Lyapunov exponent as one can see in Fig. 3(b). The average of the positive Lyapunov exponent for the ensemble of the 5 time series gives  $\bar{\lambda} = 0.371 \pm 0.001$  where the value 0.001 corresponds to the standard deviation of the five samples.

### 3. A Time Dependent Lorentz Gas.

In this section we introduce a new kind of time dependent perturbation in a Lorentz gas. We assume that the radius of the scatters are fixed and the center of mass changes according to an harmonic function  $f(t)$ , in particular we assume the case where

$$f_i(t) = \epsilon_i [1 + \cos(t)], \quad \text{for } i = x, y. \quad (16)$$

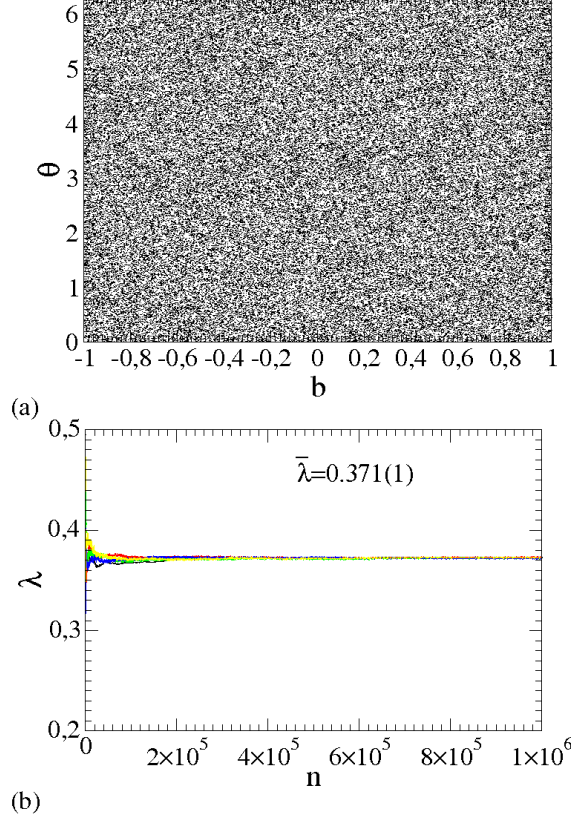


Figure 3: (a) Phase space generated from iteration of mapping (8); (b) Behaviour of the positive Lyapunov exponent of the chaotic sea. The control parameter used in both figures were  $a = 2$ .

where  $\epsilon_i$  is the amplitude of the time-dependent perturbation and  $t$  is the time. When we introduce time dependent perturbation into the model, two new dynamical variables appears, namely, velocity and time. Now, we have a two dimensional system described in terms of a four dimension nonlinear mapping which relates the collision  $n^{th}$  with the  $(n + 1)^{th}$ , i.e.,  $\Xi(\theta_n, b_n, V_n, t_n) = (\theta_{n+1}, b_{n+1}, V_{n+1}, t_{n+1})$ . The corresponding variables are: the direction of the trajectory,  $\theta_n$ ; the impact parameter,  $b_n$ ; the absolute velocity of the particle,  $V_n$  and the instant of the hit with the boundary,  $t_n$ .

Assuming that an initial condition  $(\theta_0, b_0, V_0, t_0)$  is given, we can obtain the equation that describe the dynamics of the system. Thus, according to our construction, the cartesian components of  $R$  are given by

$$X(\delta_n, t_n) = R \cos(\delta_n) + \epsilon_x [1 + \cos(t_n)], \quad (17)$$

$$Y(\delta_n, t_n) = R \sin(\delta_n) + \epsilon_y [1 + \cos(t_n)]. \quad (18)$$

where  $\delta_n$  is the angular position which is given by  $\delta_n = \pi/2 + \theta_n - \arcsin(b_n/R)$ . Since we already know the angle that the particle's trajectory does with the horizontal ( $\theta_n + \pi/2$ ) and the position

of the hit at the collision  $n^{th}$ , we can obtain the vector velocity of the particle that is written as

$$\vec{V}_n = |\vec{V}_n|[\cos(\theta_n + \pi/2)\hat{i} + \sin(\theta_n + \pi/2)\hat{j}], \quad (19)$$

where  $\hat{i}$  and  $\hat{j}$  represent the unit vectors with respect to the X and Y axis, respectively. The above expressions allow us to obtain the position of the particle as a function of time for  $t \geq t_n$ :

$$X_p(t) = X(\delta_n, t_n) + |\vec{V}_n| \cos(\theta_n + \pi/2)(t - t_n), \quad (20)$$

$$Y_p(t) = Y(\delta_n, t_n) + |\vec{V}_n| \sin(\theta_n + \pi/2)(t - t_n). \quad (21)$$

The index  $p$  denotes the corresponding coordinates of the particle. In order to know the position of the particle at  $(n + 1)^{th}$  collision we need to solve numerically the following equation

$$r = \sqrt{[X_x(t) - X_p(t)]^2 + [Y_y(t) - Y_p(t)]^2} \cong R, \quad (22)$$

where both  $X_x$  and  $Y_y$  are given by

$$X_x(t) = l_x + \epsilon_x[1 + \cos(t)], \quad (23)$$

$$Y_y(t) = l_y + \epsilon_y[1 + \cos(t)], \quad (24)$$

being  $l_x$  and  $l_y$  the X and Y components of  $l(s_n)$ ; this distance is measured from the origin of the coordinates system to the center of the  $s_n = 0, \dots, 11$  scatters at  $(n + 1)^{th}$  collision. Since we already know the position of the particle at the collision  $(n + 1)^{th}$ , one can easily find the distance between two successive impacts, which is given by  $d = \sqrt{[X_p(t) - X(\delta_n, t_n)]^2 + [Y_p(t) - Y(\delta_n, t_n)]^2}$ . Then, the time at  $(n + 1)^{th}$  collision is obtained evaluating the expression

$$t_{n+1} = t_n + \frac{\sqrt{[X_p(t) - X(\delta_n, t_n)]^2 + [Y_p(t) - Y(\delta_n, t_n)]^2}}{|\vec{V}_n|}. \quad (25)$$

The next step is to obtain the impact parameter,  $b_{n+1}$ , which is given by

$$b_{n+1} = b_n - l(s_n) \sin\left(\theta_n - \psi + \frac{\pi}{2}\right), \quad (26)$$

where  $l(s_n) = \sqrt{(\Delta X)^2 + (\Delta Y)^2}$  and  $\psi = \arctan(\Delta X/\Delta Y)$  with

$$\Delta X = l_x + \epsilon_x[\cos(t_{n+1}) - \cos(t_n)] \quad (27)$$

$$\Delta Y = l_y + \epsilon_y[\cos(t_{n+1}) - \cos(t_n)] \quad (28)$$

Moreover, the new direction of the trajectory,  $\theta_{n+1}$  is

$$\theta_{n+1} = \pi + \theta_n + 2 \arcsin\left[\frac{b_{n+1}}{R}\right]. \quad (29)$$

We already know  $(\theta_{n+1}, b_{n+1}, t_{n+1})$ , however we still have to find  $\vec{V}_{n+1}$ . At the new angular position  $\delta_{n+1}$ , the unitary tangent and normal vectors are

$$\vec{T}_{n+1} = \cos(\delta_{n+1})\hat{i} + \sin(\delta_{n+1})\hat{j}, \quad (30)$$

$$\vec{N}_{n+1} = -\sin(\delta_{n+1})\hat{i} + \cos(\delta_{n+1})\hat{j}. \quad (31)$$

Since the referential frame of the boundary is moving, then, at the instant of the collision, according to our construction, the following conditions must be matched

$$\vec{V}_{n+1} \cdot \vec{T}_{n+1} = \gamma \vec{V}_n \cdot \vec{T}_{n+1}, \quad (32)$$

$$\vec{V}_{n+1} \cdot \vec{N}_{n+1} = -\delta \vec{V}_n \cdot \vec{N}_{n+1}, \quad (33)$$

where  $\gamma \in [0, 1]$  and  $\delta \in [0, 1]$  are damping coefficients, which means that the particle can lose velocity/energy upon collision. The complete inelastic case occurs when  $\gamma = \delta = 0$ . On the other hand, when  $\gamma = \delta = 1$  corresponds to the conservative case. The upper prime indicates that the velocity of the particle is measured with respect to the moving boundary referential frame.

Hence, one can easily find that

$$\vec{V}_{n+1} \cdot \vec{T}_{n+1} = \gamma \vec{V}_n \cdot \vec{T}_{n+1} + (1 - \gamma) \vec{V}_{b(t_{n+1})} \cdot \vec{T}_{n+1}. \quad (34)$$

$$\vec{V}_{n+1} \cdot \vec{N}_{n+1} = -\delta \vec{V}_n \cdot \vec{N}_{n+1} + (1 + \delta) \vec{V}_{b(t_{n+1})} \cdot \vec{N}_{n+1}, \quad (35)$$

where  $\vec{V}_{b(t_{n+1})}$  is the velocity of the boundary which is written as

$$\vec{V}_{b(t_{n+1})} = -\sin(t_{n+1})[\epsilon_x \hat{i} + \epsilon_y \hat{j}], \quad (36)$$

Finally, the velocity at  $(n + 1)^{th}$  collision is given by

$$|\vec{V}_{n+1}| = \sqrt{(\vec{V}_{n+1} \cdot \vec{T}_{n+1})^2 + (\vec{V}_{n+1} \cdot \vec{N}_{n+1})^2}. \quad (37)$$

### 3.1. Numerical Results

Our numerical results for the time-dependent Lorentz Gas shows basically the behaviour of the average velocity of the particle. Two different procedures were applied in order to obtain the average velocity. Firstly, we evaluate the average velocity over the orbit for a single initial condition which is defined as

$$V_i = \frac{1}{n+1} \sum_{j=0}^n V_{i,j}, \quad (38)$$

where the index  $i$  corresponds to a sample of an ensemble of initial conditions. Hence, the average velocity is written as

$$\bar{V} = \frac{1}{M} \sum_{i=1}^M V_i, \quad (39)$$

where  $M$  denotes the number of different initial conditions. We have considered  $M = 1000$  in our simulations and from now on, we also fixed the value  $a = 2$ .



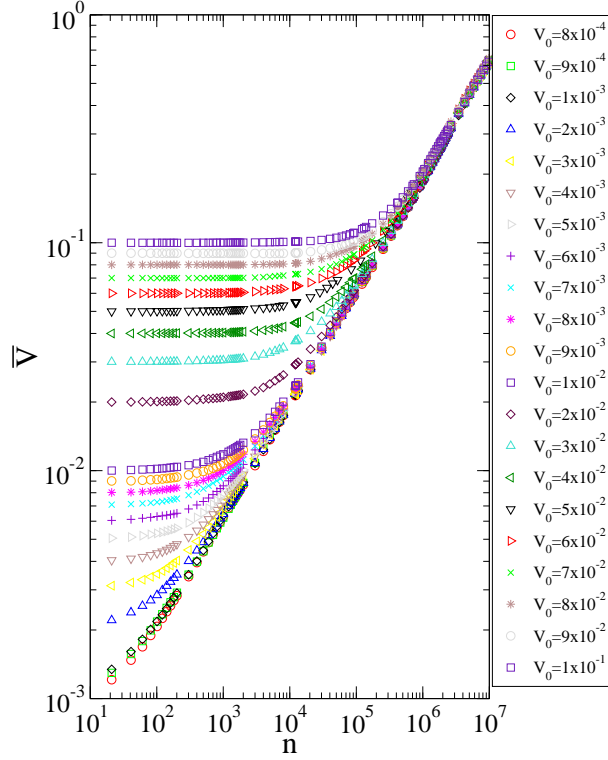


Figure 4: Behaviour of  $\bar{V} \times n$  for different initial velocities. The control parameters used were  $\epsilon_x = 10^{-4}$ ,  $\epsilon_y = 3 \times 10^{-4}$  and  $a = 2$

### 3.2. Scaling results for the conservative case

Our main goal in this section is describe a scaling present in the model for the conservative case, where, in Eq. 32 and Eq. 33, we assume  $\gamma = \delta = 1$ , and also verify the validity of LRA conjecture.

We begin discussing a scaling observed for the average velocity of the particle as function of  $V_0$  and  $n$ . It is shown in Fig. 4 the behavior of the  $\bar{V} \times n$  for different initial velocities. Hence, the control parameters used in Fig. 4 are  $\epsilon_x = 10^{-4}$ ,  $\epsilon_y = 3 \times 10^{-4}$ . Additionally, 21 different values of  $V_0$  were chosen and for each one we randomly chose  $t \in [0, 2\pi]$ ,  $\theta \in [0, 2\pi]$  and  $b \in [1 - (\epsilon_x + \epsilon_y), -1 + (\epsilon_x + \epsilon_y)]$ . As one can see, all curves of the  $\bar{V}$  behave quite similarly in the sense that: for short  $n$ , the average velocity remains constant, then after a changeover, all the curves start growing with the same exponent. Such behaviour is typical in systems that can be described using scaling approach. Based on the behavior shown in Fig. 4, we propose the following hypotheses:

1. When  $n \ll n_x$ ,  $\bar{V}$  behaves according to

$$\bar{V}_{sat} \propto V_0^{\zeta}, \quad (40)$$

2. For  $n \gg n_x$ , the average velocity is given by

$$\bar{V} \propto n^\nu, \quad (41)$$

3. The crossover iteration number that marks the change from constant velocity to growth is written as

$$n_x \propto V_0^\xi, \quad (42)$$

where  $\zeta$  and  $\nu$  are the critical exponents and  $\xi$  is a dynamic exponent.

After consider these three initial suppositions, we suppose that the average velocity is described in terms of a generalized homogeneous function of the type

$$\bar{V}(V_0, n) = l\bar{V}(l^p V_0, l^q n), \quad (43)$$

where  $l$  is the scaling factor,  $p$  and  $q$  are scaling exponents that in principle must be related to  $\zeta$ ,  $\nu$  and  $\xi$ . If we chose  $l^p V_0 = 1$ , then  $l = V_0^{-1/p}$  and Eq. (43) is given by

$$\bar{V}(V_0, n) = V_0^{-1/p} \bar{V}_1(V_0^{-q/p} n), \quad (44)$$

where  $\bar{V}_1(V_0^{-q/p} n) = \bar{V}(1, V_0^{-q/p} n)$  is assumed to be constant for  $n \ll n_x$ . Comparing Eq. (44) and Eq. (40), we obtain  $\zeta = -1/p$ .

On the other hand, Choosing now  $l = n^{-1/q}$ , Eq. (43) is rewritten as

$$\bar{V}(V_0, n) = n^{-1/q} \bar{V}_2(n^{-p/q} V_0), \quad (45)$$

where the function  $\bar{V}_2$  is defined as  $\bar{V}_2(n^{-p/q} V_0) = \bar{V}(n^{-p/q} V_0, 1)$ . It is also assumed to be constant for  $n \gg n_x$ . Comparing Eq. (45) and Eq. (41) we find  $\nu = -1/q$ . Given the two different expressions of the scaling factor  $l$ , we obtain a relation for the dynamic exponent  $\xi$ , which is given by

$$\xi = \frac{\zeta}{\nu}. \quad (46)$$

Note that the scaling exponents are determined if the critical exponents  $\zeta$  and  $\nu$  were numerically obtained. The exponent  $\nu$  is obtained from a power law fitting for the average velocity when  $n \gg n_x$ . Thus, an average of these values gives  $\nu = 0.49(1)$ . Figure 5 shows the behaviour of (a),  $\bar{V}_{sat} \times V_0$  and (b),  $n_x \times V_0$ . Applying power law fittings we obtain  $\zeta = 1.00(1) \cong 1$  and  $\xi = 2.01(3)$ . Considering the previous values of both  $\zeta$  and  $\nu$  and using  $\xi = \zeta/\nu$ , we find that  $\xi = 2.04(2)$ . Such result indeed agrees with our numerical data. In order to confirm the initial hypotheses and, since the values of the scaling exponents  $\zeta$ ,  $\nu$  and  $\xi$  are now known, we will collapse all the curves onto a single and universal plot, as demonstrated in Fig. 6. Additionally, such result allow us to confirm the validity of LRA conjecture since the  $\bar{V}$  grows unbounded for  $n \gg n_x$ .

### 3.3. Scaling results for the dissipative case.

In this section we will use the same scaling formalism as used in the previous section. We concentrate to characterize the behaviour of the average velocity in terms of the number of collisions with the boundary and as a function of the damping coefficient along the normal component

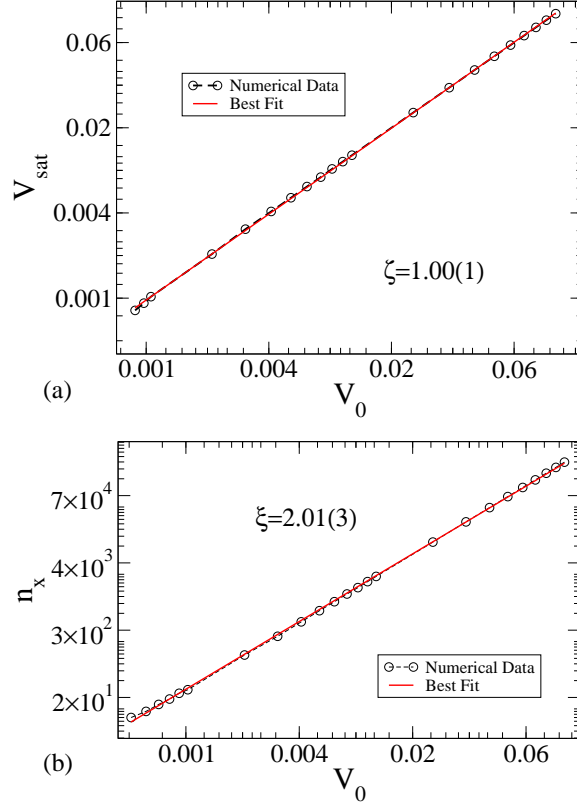


Figure 5: (a) Plot of  $V_{\text{sat}} \times V_0$ . (b) Behaviour of  $n_x$  as function of  $V_0$ .

of the particle's velocity,  $\delta$ . We study a dissipative version of the Lorentz Gas close to the transition from unlimited to limited energy growth. Indeed, such a transition happens when the control parameter  $\delta \rightarrow 1$  and it is better characterized if adopt the following transformation  $\delta \rightarrow (1 - \delta)$ . To obtain the average velocity, each initial condition has a fixed initial velocity,  $V_0 = 10^{-4}$  and randomly chose  $t \in [0, 2\pi]$ ,  $\theta \in [0, 2\pi]$  and  $b \in [1 - (\epsilon_x + \epsilon_y), -1 + (\epsilon_x + \epsilon_y)]$ . The control parameter  $\gamma$  were fixed as been  $\gamma = 1$ .

It is shown in Fig. 7 the behaviour of average velocity as function of the number of collision for different values of  $\delta$ . Note that, for different values of  $\delta$ , the average velocity, for small  $n$ , starts to grow with the same slope and them they bend towards a regime of saturation for long enough values of  $n$ . The changeover from growth to the saturation is marked by a typical crossover number  $n_x$ . For such a behaviour, we can propose the following scaling hypotheses:

1. When  $n \ll n_x$  the average velocity is

$$\bar{V} \propto n^\eta, \quad (47)$$

2. For long time,  $n \gg n_x$ , the average velocity approaches a regime of saturation, that is

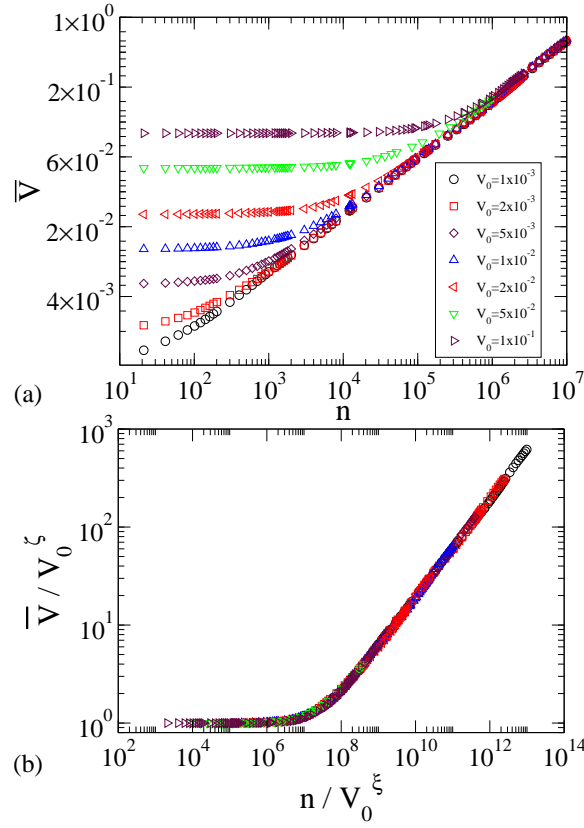


Figure 6: (a) Behaviour of average velocity for different values of  $V_0$ ; (b) their collapse onto a single and universal plot.

described as

$$\bar{V}_{sat} \propto (1 - \delta)^\sigma, \quad (48)$$

3. The crossover number that marks the regime of growth to the constant velocity is written as

$$n_x \propto (1 - \delta)^z, \quad (49)$$

where  $\sigma$ ,  $\eta$  and  $z$  are critical exponents.

These scaling hypotheses allow us to describe the average velocity in terms of a scaling function of the type

$$\bar{V}[n, (1 - \delta)] = l \bar{V}[l^p n, l^q (1 - \delta)], \quad (50)$$

where  $p$  e  $q$  are scaling exponents and  $l$  is a scaling factor. Since  $l$  is a scaling factor, we can chose it such that  $l^p n = 1$ , yielding

$$\bar{V}[n, (1 - \delta)] = n^{-1/p} \bar{V}_1[(n)^{-q/p} (1 - \delta)], \quad (51)$$

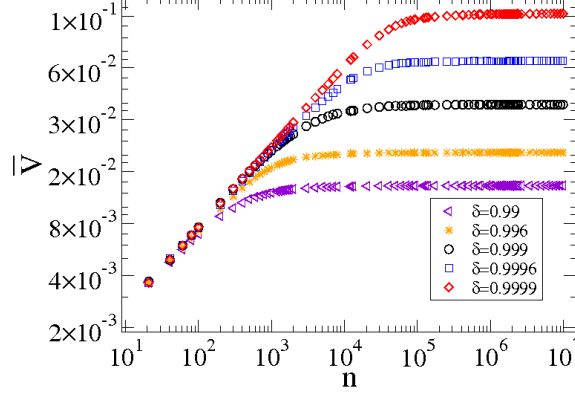


Figure 7: Behaviour of  $\bar{V} \times n$  for different values of  $\delta$ , as labeled in the figure.

where  $\bar{V}_1[(n)^{-q/p}(1-\delta)] = \bar{V}[1, (n)^{-q/p}(1-\delta)]$  is assumed to be constant for  $n \ll n_x$ . Comparing Eqs. (47) and (51), we obtain  $\eta = -1/p$ . A power law fitting gives us that  $\eta = 0.471(2)$ . Such value was obtained from the range of  $\delta \in [0.99, 0.99999]$ . Choosing now  $l^q(1-\delta) = 1$ , we have that  $l = (1-\delta)^{-1/q}$  and Eq. (50) is rewritten as

$$\bar{V}[n, (1-\delta)] = (1-\delta)^{-1/q} \bar{V}_2[(1-\delta)^{-p/q}n], \quad (52)$$

where  $\bar{V}_2[(1-\delta)^{-p/q}n] = \bar{V}[(1-\delta)^{-p/q}n, 1]$  is assumed to be constant for  $n \gg n_x$ . Comparing Eqs. (48) and (52), we obtain  $-1/q = \sigma = -0.47(3)$  [see Fig. 8 (a)]. Using now the expressions obtained for the scaling factor  $l$ , we can easily show that

$$z = \frac{\sigma}{\eta} = 0.99(5), \quad (53)$$

which is quite close to the value obtained numerically, as shown in Fig. 8 (b). A confirmation of the initial hypotheses is made by a collapse all the curves of  $\bar{V} \times n$  onto a single and universal plot, as shown in Fig. 9, showing that the system is scaling invariant. We also shown that dissipation causes a drastic change in the behavior of  $\bar{V}$ . Note that when  $\delta \rightarrow 1$ , implies that Eq. 48 and Eq. 49 diverge, thus recovering the results for the conservative case, i.e., Fermi acceleration. However, when  $\delta$  is slightly less than 1, the average velocity grows and then reach a regime of saturation for long enough time. Our results reinforce that dissipation introduced via damping coefficients is a sufficient condition to suppress the phenomenon of Fermi acceleration.

#### 4. Conclusion

In this paper we consider the problem of a classical Lorentz Gas considering both the static and time-dependent boundary. For the static case we obtain the mapping that describes the dynamics of the system and we have shown that the model has a chaotic component characterized with positive Lyapunov Exponent. After that, we introduce a new type of the time-dependent perturbation on the boundary. Our results confirm the validity of LRA conjecture for the conservative case since the phenomenon of Fermi acceleration is observed. When dissipation, via

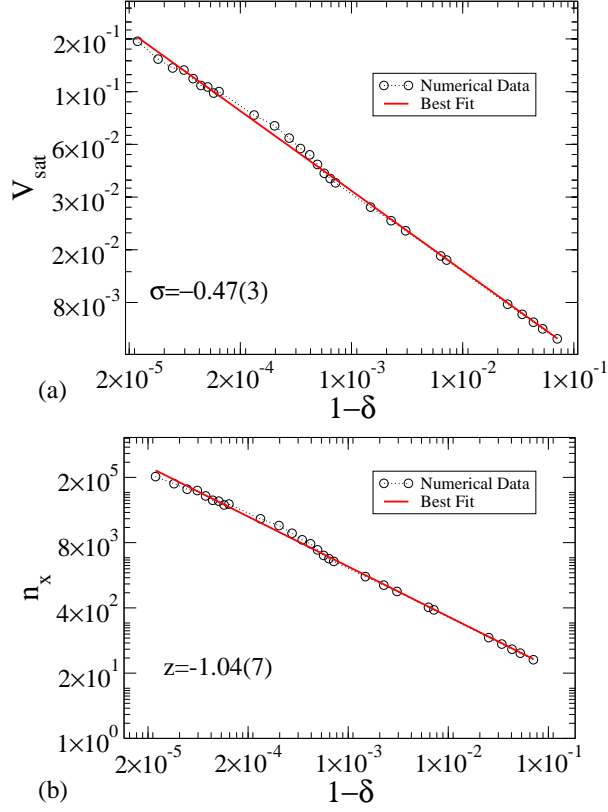


Figure 8: (a) Behaviour of  $\bar{V}_{\text{sat}} \times (1 - \delta)$ . (b) Behaviour of the crossover number  $n_x$  against  $(1 - \delta)$ . A power law fitting in (a) furnishes  $\sigma = -0.47(3)$  while in (b)  $z = -1.04(7)$ .

damping coefficients, is introduced into the model we observed that the average velocity grows with time and then reaches a constant value for large enough time confirming that Fermi acceleration is suppressed. Finally, the average quantities were described by scaling functions with characteristic exponents whose validity was confirmed with the collapse of the curves of  $\bar{V}$  into an universal plot.

## ACKNOWLEDGMENTS

D.F.M.O gratefully acknowledges Max Planck Institute for financial support. E. D. L. is grateful to FAPESP, CNPq and FUNDUNESP, Brazilian agencies. The authors acknowledge Dr. Douglas Fregolente for a careful reading on the manuscript.

## References

- [1] E. Fermi, On the Origin of the Cosmic Radiation, Phys. Rev. 75 (1949) 1169.

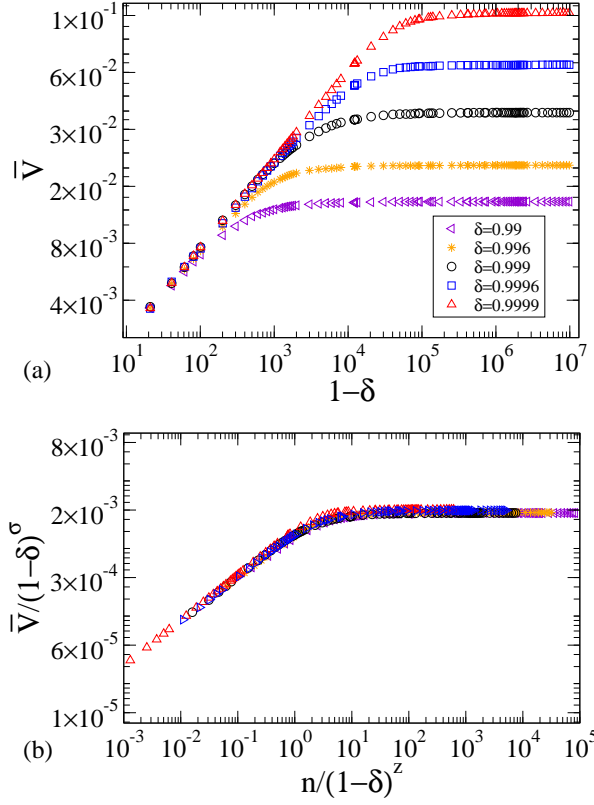


Figure 9: (a) Different curves of the  $\bar{V}$  for five different control parameters. (b) Their collapse onto a single and universal plot.

- [2] S. E. Sklarz, D. J. Tannor, N. Khaneja, Decoherence Control by Tracking a Hamiltonian Reference Molecule, *Phys. Rev. A* 69 (2004) 053408.
- [3] R. Gommers, S. Bergamini, F. Renzoni, Dissipation-Induced Symmetry Breaking in a Driven Optical Lattice, *Phys. Rev. Lett.* 95 (2005) 073003.
- [4] M. Steiner, M. Freitag, V. Perebeinos, J. C. Tsang, J. P. Small, M. Kinoshita, D. Yuan, J. Liu, P. Avouris, Phonon populations and electrical power dissipation in carbon nanotube transistors, *Nature Nanotechnology* 4 (2009) 320.
- [5] K. Nakamura and T. Harayama, *Quantum Chaos and Quantum Dots*, Oxford University Press, Oxford, 2004.
- [6] D.G. Ladeira, J.K.L. da Silva, Time-dependent properties of a simplified Fermi-Ulam accelerator model, *Phys. Rev. E* 73 (2006) 026201.
- [7] Leonel, E.D., J.K.L. da Silva, S.O. Kamphorst, On the dynamical properties of a Fermi accelerator model, *Physica A* 331 (2004) 435.
- [8] A.K. Karlis, P.K. Papachristou, F.K. Diakonou, V. Constantoudis, P. Schmelcher, Hyperacceleration in a Stochastic Fermi-Ulam Model, *Phys. Rev. Lett.* 97 (2006) 194102.
- [9] A.K. Karlis, P.K. Papachristou, F.K. Diakonou, V. Constantoudis, P. Schmelcher, Fermi acceleration in the randomized driven Lorentz gas and the Fermi-Ulam model, *Phys. Rev. E* 76 (2007) 016214.
- [10] J.V. José, R. Cordery, Study of a quantum fermi-acceleration model, *Phys. Rev. Lett.* 56 (1986) 290.
- [11] E.D. Leonel, D.F.M. Oliveira, R.E. Carvalho, Scaling properties of the regular dynamics for a dissipative bouncing ball model. *Physica A* 386 (2007) 73.
- [12] D.F.M. Oliveira, E.D Leonel, The Feigenbaum's  $\delta$  for a high dissipative bouncing ball model. *Brazilian Journal of*

- Physics 38 (2008) 62.
- [13] A. D. Pustynnikov, Construction of periodic-solutions in an infinite system of fermi-pasta-ulam ordinary differential-equations, stability, and KAM Theory. *Theor. Math. Phys.* 50 (1995) 449.
  - [14] A. D. Pustynnikov, On Ulam Problem, *Theor. Math. Phys.* 57 (1983) 1035.
  - [15] P.J. Holmes, The dynamics of repeated impacts with a sinusoidally vibrating table, *J. Sound and Vibr.* 84 (1982) 173.
  - [16] R.M. Everson, Chaotic dynamics of a bouncing ball, *Physica D* 19 (1986) 355
  - [17] G.A. Luna-Acosta, Regular and chaotic dynamics of the damped Fermi accelerator, *Phys. Rev. A* 42 (1990) 7155.
  - [18] E.D. Leonel, A.L.P. Livorati, Describing Fermi acceleration with a scaling approach: bouncer model revisited, *Physica A* 387 (2008) 1155.
  - [19] T.L. Vincent, A.I. Mees, Controlling a Bouncing Ball, *Journal of Bifurcation and Chaos* 10 (2000) 579.
  - [20] A.C.J. Luo, An unsymmetrical motion in a horizontal impact oscillator, *ASME J. Vib. Acoust.* 124 (2002) 420.
  - [21] A.C.J. Luo, R.P.S. Han, The dynamics of a bouncing ball with a sinusoidally vibrating table revisited, *Nonlinear Dynamics* 10 (1996) 1.
  - [22] A. J. Lichtenberg, M.A. Lieberman, R. H. Cohen, Fermi acceleration revisited, *Physica D: Nonlinear Phenomena*, 1, (1980) 291.
  - [23] A. J. Lichtenberg, M.A. Lieberman, *Regular and Chaotic Dynamics.* (Appl. Math. Sci. 38, Springer Verlag, New York, 1992.
  - [24] A. Loskutov, A.R. Ryabov, L.G. Akinshin, Properties of some chaotic billiards with time-dependent boundaries *J. Phys. A: Math. Gen.* 33 (2000) 7973.
  - [25] E. D. Leonel, D. F. M. Oliveira, A. Loskutov, Fermi acceleration and scaling properties of a time dependent oval billiard. *Chaos*, 19, (2009) 033142.
  - [26] A. B. Ryabov, A. Loskutov, Time-dependent focusing billiards and macroscopic realization of Maxwell's Demon. *Journal of Physics. A, Mathematical and Theoretical*, 43 (2010) 125104.
  - [27] D. F. M. Oliveira, E. D. Leonel. Boundary crisis and suppression of Fermi acceleration in a dissipative two dimensional non-integrable time-dependent billiard. *Physics letters A*, 2010.
  - [28] E. D. Leonel, Breaking down the Fermi acceleration with inelastic collisions, *Journal of Physics A, Mathematical and General*, 40 (2007) F1077.
  - [29] D. G. Ladeira, J. K. L. da Silva, Scaling features of a breathing circular billiard. *Journal of Physics. A, Mathematical and Theoretical*, 41 (2008) 365101.
  - [30] E. D. Leonel, Breaking down the Fermi acceleration with inelastic collisions, *J. Phys. A: Math. Theor.* 40 (2007) F1077.
  - [31] D. G. Ladeira, E. D. Leonel, Competition between suppression and production of Fermi acceleration. *Physical Review. E, Statistical, Nonlinear, and Soft Matter Physics*, 81 (2010) 036216.
  - [32] J.P. Eckmann, D. Ruelle, Ergodic theory of chaos and strange attractors, *Rev. Mod. Phys.* 57 (1985) 617.